Tunneling spectroscopy study and modeling of electron transport in small conjugated azomethine molecules

J. J. W. M. Rosink,* M. A. Blauw, L. J. Geerligs, E. van der Drift,† and S. Radelaar‡
Delft Institute of Microelectronics and Submicron Technology and Department of Applied Physics, Delft University of Technology, P.O. Box 5046, 2600 GA Delft, The Netherlands
(Received 6 December 1999)

Scanning tunneling spectroscopy results are presented on oriented monolayer films of conjugated phenyl-based molecules self-assembled on gold. Three related molecules of different lengths are investigated. The molecules do not show resonances in electron transmission at least up to 1.5 V. We model the experiments successfully by the molecules acting as a potential barrier to electron transmission. The potential barrier is trapezoidal when the molecule has a permanent dipole moment (normal to the gold surface), in agreement with the asymmetric $I(V)$ curves. For 2 V bias and larger, the film is modified by the measurement, which prevents measurements of possible resonances at higher energies.

I. INTRODUCTION

The electronic transport properties of organic π-conjugated molecules have been the subject of many recent studies, both theoretical and experimental. Different experimental ways have been pursued to investigate conduction through molecules, which can be grouped in two approaches: contacting isolated single molecules or molecules in thin (usually monolayer) films,[1,2] or studying transport in thick films and devices, such as organic thin-film transistors or light emitting diodes.[3]

A major goal in this research on molecular electronics is to study the transport along the π orbitals *inside* the molecular chain. The natural approach is to try to obtain an isolated molecule between two electrical contacts, which is obviously very difficult to realize and especially difficult to verify. Alternatively, a well-ordered system where the molecules are aligned can be used. Scanning tunneling microscopy (STM) experiments have proven to be a very suitable tool for the investigation of ordered monolayer films. The STM allows electrical contacting of one or a few molecules at a time.[1] In the same experiment, it allows imaging of the structural characteristics of the film.

In this work, we have used the STM to study small phenyl-based molecules (oligomers), which have been grown from their constituting monomers on gold substrates.[4] The STM acts as a contact on the ''top'' side of the film to one or a few molecules. The supporting gold substrate acts as the other (''bottom'') contact. The monomers are basically single benzene derivatives with two functional groups in the para position. In the growth process these groups react and link the conjugated rings together, and extend the conjugation over the whole length of the resulting molecule. This process results in a monolayer film of molecular wires, aligned upwards with respect to the substrate (see Fig. 1).

This paper presents scanning tunneling spectroscopy measurements (STS) and their interpretation. Our measurements are off-resonance with respect to the molecular orbitals, i.e., electrons tunnel at energies in the gap between the HOMO (highest occupied molecular orbital), and the LUMO (lowest unoccupied molecular orbital). If the distance from the Fermi level to the HOMO and LUMO is large, a simple Wentzel-Kramers-Brillouin (WKB) approach for tunneling of electrons[5] will be applicable. This means that the molecule acts as a tunneling barrier between two metal electrodes. We will motivate and use a model that, apart from the tunneling distance, includes only the barrier height on both sides of the barrier. Dhirani *et al.* used a similar approach, based on the ''band picture'' of the molecules, where the position of HOMO and LUMO determine the height of the tunnel barrier.[6] Additionally, in Ref. 6, charge transfer from metal to molecule was introduced as having influence on the shape of the tunnel barrier.

In this paper we show that permanent dipole moments of the molecules appear to be a dominant ingredient for barrier

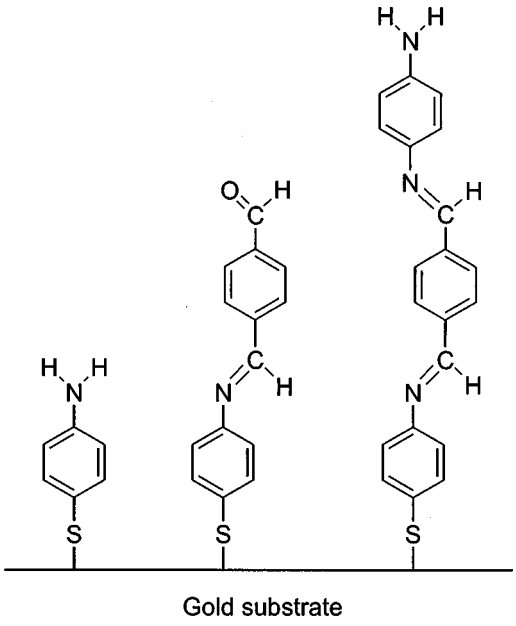

FIG. 1. Schematic picture of the molecules under investigation after their growth from solution by self-assembly. From left to right: 4-ATP, AT, and ATD. Abbreviations and deposition procedure are described in the text.

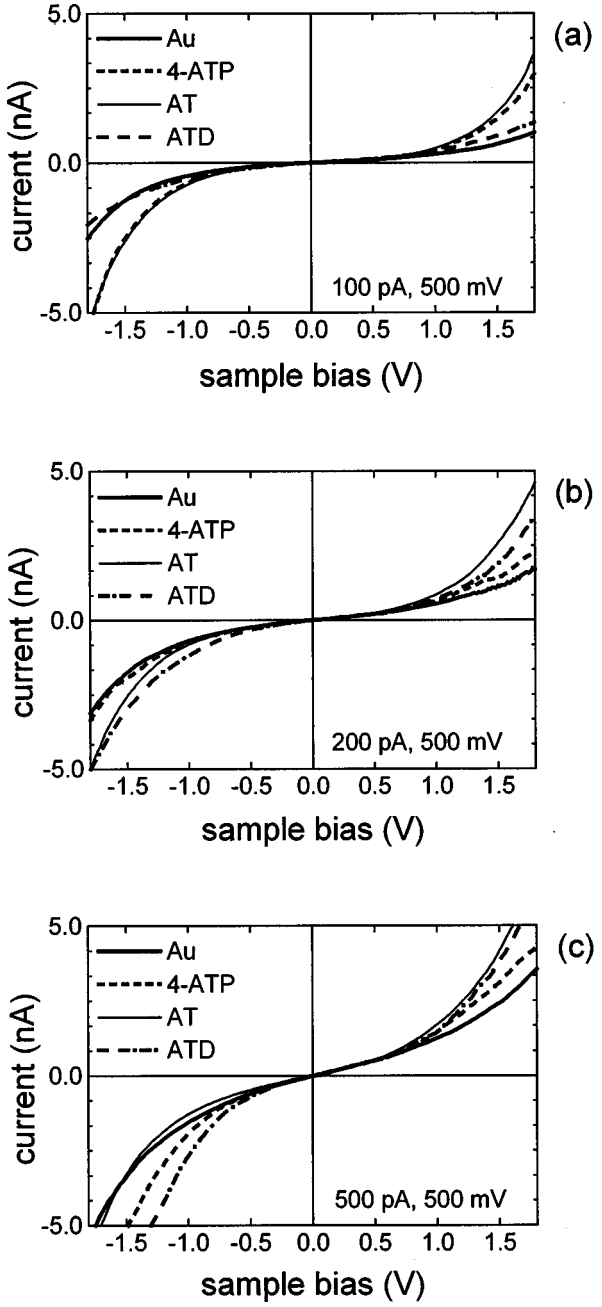

FIG. 2. Experimental *I-V* curves at a bias of 500 mV for a setpoint of (a) 100 pA (5 GΩ), (b) 200 pA (2.5 GΩ), and (c) 500 pA (1 GΩ). Each curve is an average of 60–70 % of 1024 curves, taken at a single spot on the sample in a nitrogen atmosphere.

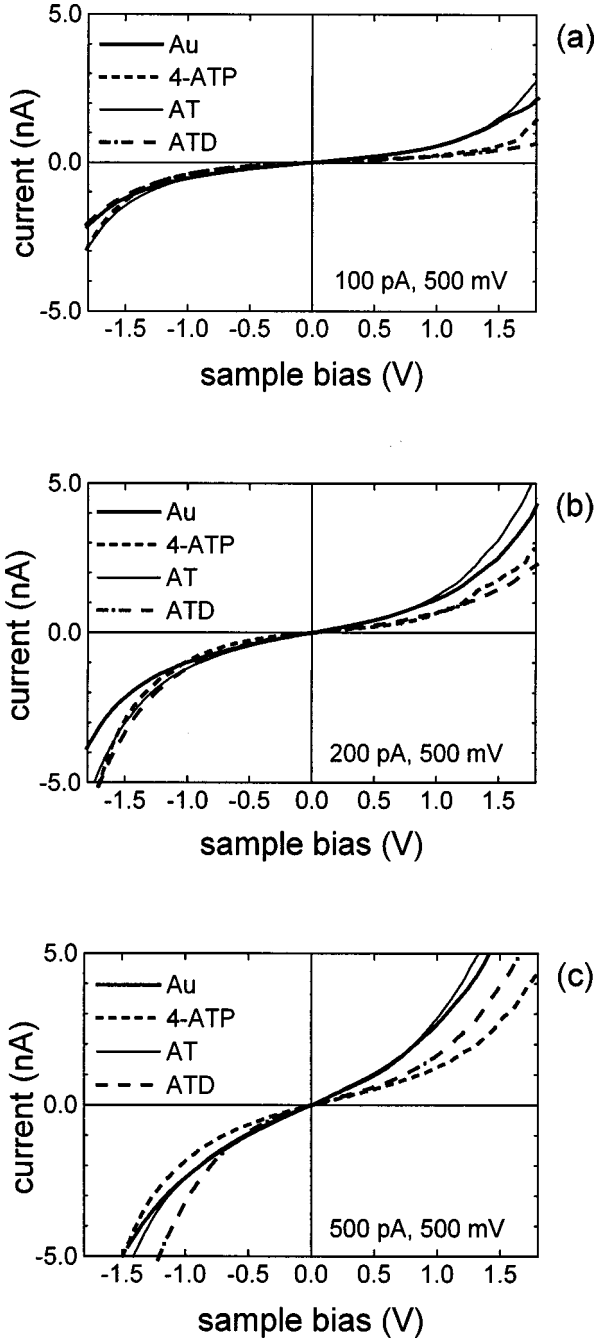

FIG. 3. Experimental *I-V* curves at a bias of 50 mV for a setpoint of (a) 100 pA (5 GΩ), (b) 200 pA (2.5 GΩ), and (c) 500 pA (1 GΩ). Each curve is an average of 60–70 % of 1024 curves taken on a regular grid of 100 nm^2, in air.

shape and height as found by analysis of asymmetry of the STS $I(V)$ curves. This is consistent with work by Campbell *et al.*,[7] who investigated monolayers with permanent dipole moments as a means to suppress metal-organic Schottky barriers. In the model that we use in this paper, the voltage drop is distributed proportionally over the barrier. In a picture where the molecular properties are taken into account in more detail, the possibility that the chemical potential of the molecule is more fixed to the substrate is considered.[8,9]

This paper is organized as follows. In Sec. II, we give the experimental details of the growth of the molecular layers, and results of the scanning tunneling spectroscopy. In Sec. III, we describe the theoretical model for our experiments. In Sec. IV, we discuss the fits of the model to the experimental results in the context of the properties of the molecules and results from literature.

II. EXPERIMENT

Gold substrates were prepared by depositing a thin-film (100 nm) of gold on thermally oxidized (200 nm) silicon. The organic molecules were grown *in situ* from solution as self-assembled monolayer films, by immersing the substrate sequentially in solutions of different monomers. Each immersion step results in the addition of a new monolayer film

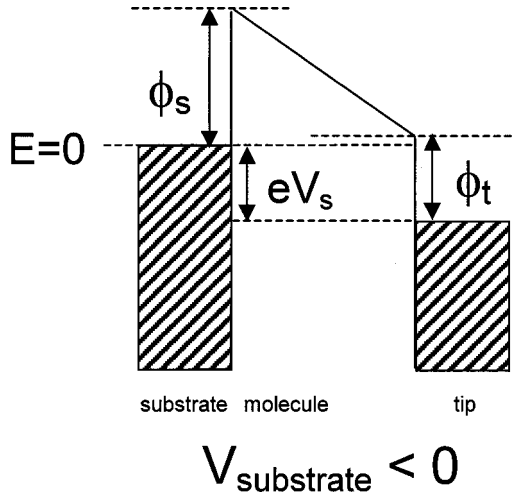

FIG. 4. Tunnel barrier profile used to model our STS experiments. E is the integration parameter in Eq. (4), running from 0 to eV.

by selective chemisorption. The monomers are benzene derivatives with two functional groups (-SH, -NH_2 or -CHO) in the para position: 4-aminothiophenol (4-ATP), terephthaldicarboxaldehyde (TDA), and 1,4-diaminobenzene (DAB). Monomers in this film react with the underlying layer resulting in either a covalent bond with the gold substrate by means of a thiol endgroup (Au-S-R first layer), or an imine bond (R-C═N-R′, following layers). No crosslinking can occur. Once all sites are occupied, excess molecules from the solution are physisorbed only and can be gently removed by rinsing in the pure solvent. Figure 1 shows the molecules that have been studied in this paper. We use the following abbreviations: for one aromatic ring: 4-ATP, for two rings: AT, and for three rings: ATD. The aromatic rings are linked together through carbon-nitrogen double bonds (the imine bonds). π conjugation extends over all atoms but the coupling with the sulfur is reduced.[9] By angle-dependent x-ray photoelectron spectroscopy measurements, in which the elemental composition as a function of depth was followed, and by ellipsometry, in which the thickness as a function of the number of monomer layers was followed, we have confirmed that the molecules are oriented approximately perpendicular to the substrate. A detailed description and analysis of the growth process is given elsewhere.[4]

STM measurements were performed with a Digital Instruments Nanoscope IIIa system with a TipView STM head using freshly cut Pt/Ir tips. Both topographic and spectroscopic data [current-voltage, $I(V)$, taken with interrupted feedback loop] were obtained. With STM, for very small voltage (10–50 mV) and large current ($\sim$ 1 nA) we observed a $\sqrt{3}\times\sqrt{3}$ reconstructed [compared to the Au(111)1×1] surface topography, which we associate with the sulfur atoms bonded to the Au(111) surface. The molecules order in a hexagonal pattern in a $(\sqrt{3}\times\sqrt{3})$R30° structure with a nearest-neighbor spacing of 4.9 ± 0.3 Å, and a corresponding coverage of 4.8×10^{18} molecules/m^2.[10] However, with STM at a low bias current, we did not observe crystal-like domains, such as monolayers of long-alkanethiol molecules usually show. Topographic images show a considerable difference between the bare gold substrates and samples with molecular films. In the latter case, the formation of pits is often observed. In the literature, the occurrence of these pits is attributed to etching of the underlying gold layers due to the reaction of thiol-groups with gold atoms, forming dissolvable complexes.[11] Noise, in the form of height fluctuations, is larger in topographic images of films than of bare gold.

$I(V)$ spectra were taken for different feedback voltage and current setpoints, i.e., for different initial sample-tip distances. Tunnel resistances were in the range 1–10 GΩ; current setpoints between 50 and 500 pA at 500 mV voltage bias. Experiments were performed both in air and dry nitrogen ambient, without clear systematic differences. 1024 consecutive $I(V)$ sweeps were taken on a gold (111) terrace, at a fixed position on the terrace or at a regular grid of 100 nm^2. $I(V)$ data presented in this paper represent the average of a subset from the collected $I(V)$ curves, where only those were included in the averaging that were going through the setpoint, within a factor of 0.8 to 1.2 or 0.7 to 1.5 of the setcurrent, to select curves which were not affected much by drift of the STM ($\pm$60–70 % of all curves).[12] Assuming mostly fluctuations in the z movement of the tip as the source of noise in the $I(V)$, we have averaged $\ln(I)$ vs V. The polarity of the bias voltage is defined in the conventional way as representing the voltage on the substrate. This means that for negative sample bias voltage, electrons tunnel from sample to STM tip.

Figure 2 shows $I(V)$ curves taken on a single spot in nitrogen atmosphere. Figure 3 shows $I(V)$ curves taken on a regular grid of 100 nm^2 in air. All displayed curves are averaged in the way described above. The curves are nonlinear, which we interpret below as due to the exponential increase of transmission through a tunnel barrier when it is distorted by an applied voltage. Remarkably, tunneling spectra for all 4-ATP and ATD films show asymmetric behavior, whereas for all AT films the curves are approximately symmetric. For a bare-gold surface the asymmetry varied, with some $I(V)$ curves symmetric and some asymmetric. The asymmetry in all experiments was always with higher current for negative sample bias.

III. THEORY AND MODEL

Figure 4 shows the potential landscape used in our simplified representation of a metal-molecule-metal sandwich. The tilted (trapezoidal) barrier, which was numerically investigated by Brinkman *et al.*,[13] is the simplest potential (with the smallest number of parameters) which in itself can describe our results of asymmetric $I(V)$ curves. This potential profile is a realistic physical representation if there is low transmission and the tunneling electron is a significant distance away from resonance with any molecular orbital. (From the absence of resonances in the experimental $I(V)$ curves, we deduce that this distance is at least 1.5 eV.) In that situation there is no strong distinction between the picture that the electron occupies the molecular density of states (DOS), which is exponentially small at the Fermi level, and the picture that the molecule acts as a potential barrier, so the electron tunnels through the molecule. In both cases, the transmission of an electron can be approximately described by the WKB approach of a decaying wave function.[14]

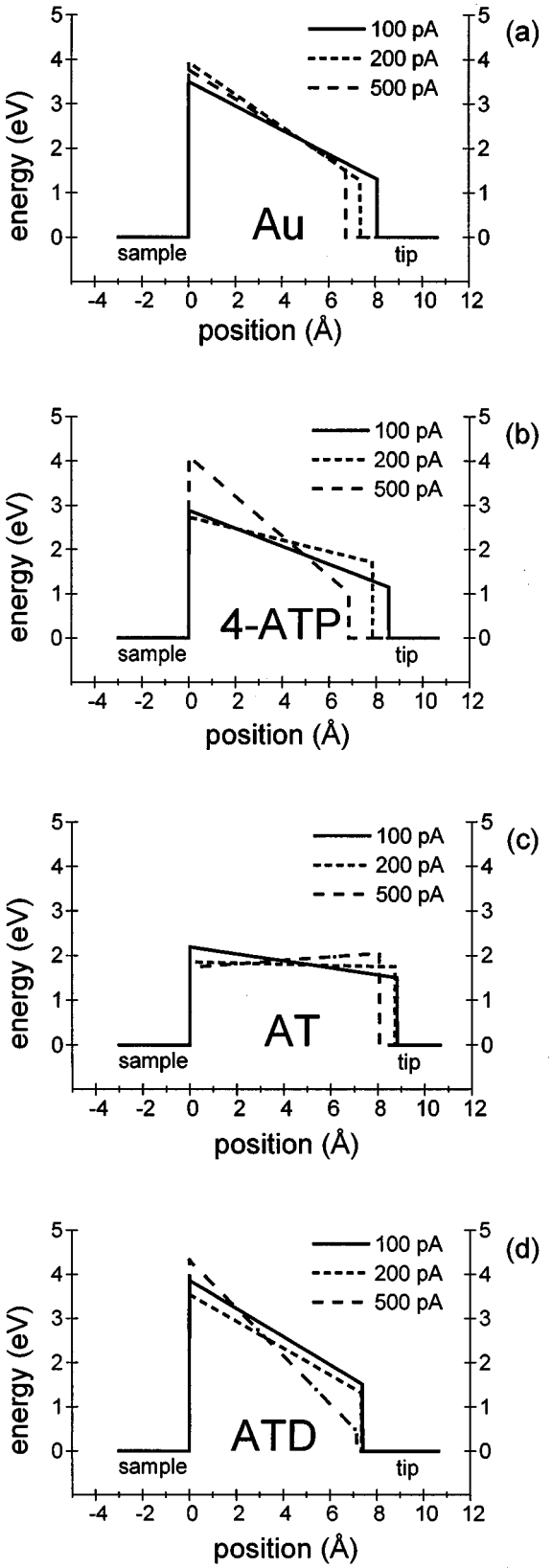

FIG. 5. Tunnel barrier profile as determined from fits to measurements in Fig. 2, according to Eq. (4): (a) Au, (b) 4-ATP, (c) AT, and (d) ATD.

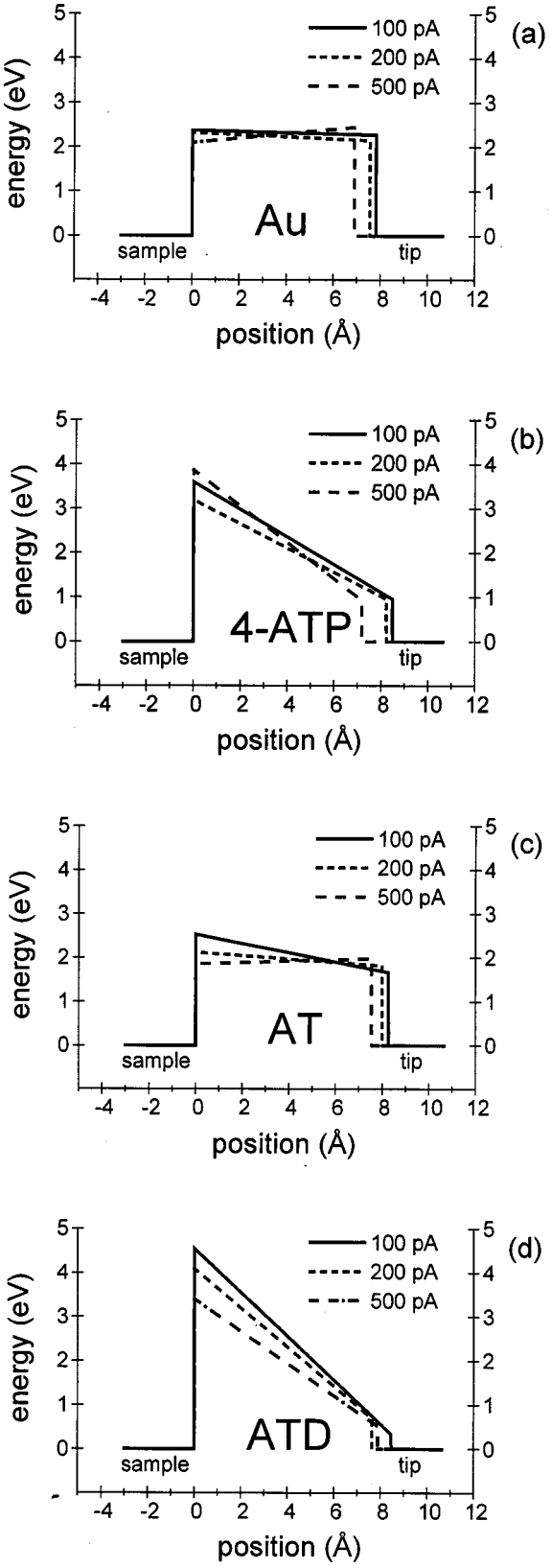

FIG. 6. Tunnel barrier profile as determined from fits to measurements in Fig. 3: (a) Au, (b) 4-ATP, (c) AT, and (d) ATD.

Of course, in the latter picture the barrier height is an effective quantity. We neglect the precise characteristics of the DOS in the molecule (position and width of the various orbitals), which are all summarized in the model parameters. It is expected that one orbital will dominate for the transmission, probably HOMO or LUMO, whichever is closest to the Fermi level, although the spatial extension of the orbitals will have some influence here.[8] We also neglect the details of

TABLE I. Results from Fig. 2: Parameters resulting from fits to trapezoidal barrier model. Errors in the last digit are given in parentheses after the fitted value.

	500 mV, 100 pA			500 mV, 200 pA			500 mV, 500 pA		
Sample	ϕ_t (eV)	ϕ_s (eV)	s (Å)	ϕ_t (eV)	ϕ_s (eV)	s (Å)	ϕ_t (eV)	ϕ_s (eV)	s (Å)
Au	1.31(1)	3.50(4)	8.07(2)	1.28(1)	3.94(7)	7.35(4)	1.56(1)	3.77(5)	6.73(3)
4-ATP	1.15(3)	2.88(11)	8.55(5)	1.71(3)	2.73(14)	7.85(7)	1.02(2)	4.10(12)	6.84(5)
AT	1.50(2)	2.19(10)	8.82(8)	1.74(1)	1.85(4)	8.73(3)	2.05(1)	1.73(3)	8.07(2)
ATD	1.51(4)	3.86(25)	7.40(9)	1.32(4)	3.54(25)	7.35(10)	0.46(3)	4.32(11)	7.15(6)

the potential barrier at the interfaces of molecule and metal electrodes, for which exact treatment would require quantum chemical calculations of which the accuracy will be difficult to assess.

The tilt of the barrier is the essential ingredient for producing an asymmetric curve. This tilt can have a threefold origin. First, it can be due to different work functions of the gold substrate and the Pt/Ir STM tip, second, the barrier can be geometrically asymmetric, and third, it can be due to a permanent dipole in the molecule (and perhaps other dipoles, at the tip or gold surface) as was shown by Campbell *et al.*[7]

We derived the tunneling current according to the WKB approximation for this potential landscape. The starting expression is[15,16]

$$I(V)=\frac{2e}{h}\int_0^{eV} dE\,\rho_t(E-eV)\rho_s(E)T_0(E,V), \qquad (1)$$

where T_0 is the transmission probability as a function of energy and the prefactor $2e/h$ is an approximation which assumes one-dimensional-quantized conductance between two states which match in energy and have $T_0=1$. $\rho_t(E)$ and $\rho_s(E)$ are the local DOS of the tip and sample at an energy E referred to the Fermi level, e is the unit charge, with $e>0$, and V is defined as V_{sample}-V_{tip} as is the convention in STM experiments (tip is grounded). In here, we also take a zero-temperature approximation, which is allowed because k_BT is only 25 meV compared to our experimental scale of 1.5 V.

The transmission through the molecule (the barrier) is in the WKB approximation given by the temperature-independent-transmission probability $T_0(E,V)$:[17]

$$T_0(E,V)=\exp\left\{-\int_0^s dz\left(\frac{8m}{\hbar^2}[U(z)-E]\right)^{1/2}\right\}. \qquad (2)$$

Here, $U(z)$ describes the potential profile between tip and substrate, referred to as the sample Fermi energy. For a tilted potential barrier, the parameters are the tunnel barrier at the molecule-sample side (ϕ_s), the tip-side (ϕ_t), and the total distance between tip and sample (s):

$$U(z)=\phi_s+(\phi_t-\phi_s+eV)\cdot\frac{z}{s}, \qquad (3)$$

where z runs from sample to tip ($z=0,\ldots,s$). Assuming a uniform DOS ($\rho_t=\rho_s=1$), Eqs. (1)–(3) can be combined to obtain an expression for the tunneling current as a function of applied bias voltage V:

$$I(V)=\frac{2e^2}{h}\int_0^{eV} dE \times\exp\left\{-\int_0^s dz\left[\frac{8m}{\hbar^2}\left(\phi_s+(\phi_t-\phi_s+eV)\frac{z}{s}-E\right)\right]^{1/2}\right\} \qquad (4)$$

which we will use to fit the experimental $I(V)$ curves (we put $U-E\equiv 0$ for $U<E$). We will take $m=m_e$ (a deviation would correspond to a scaling of the energies and/or the thickness s of the potential profile).

Note that we have neglected any possible structure in the DOS of the Au substrate or Pt/Ir tip. We think this is validated by the measurements on bare gold and we will come back to this at the end of the next section.

IV. DISCUSSION

4-ATP and ATD show strongly asymmetric $I(V)$ curves with a higher current for negative sample bias. AT consistently shows roughly symmetric $I(V)$ curves. Bare gold shows varying results. The potential profiles responsible for this behavior, resulting from fits of Eq. (4) to the experiments, are depicted in Figs. 5 and 6. In Tables I and II, the fit parameters ϕ_s, ϕ_t, and s are shown. Figure 7 shows that the fitted curves are in good agreement with the experimental results.

Apparently there is an important variation in molecule properties between 4-ATP and ATD on the one hand, and AT on the other hand, which is reflected in the tilt of the fitted potential barrier. A related effect has been investigated before, for self-assembled monolayers of nonconjugated molecules, by Campbell *et al.*[7] They established that molecular dipole moments result in a change in surface work function. If this work-function change is distributed linearly over the length of the molecule, a sloped potential profile is obtained as in our model. The magnitude of the change $\Delta\phi$ can be calculated from the molecular dipole moment, in a simple parallel plate approximation. For internal dipole moment $\mu_\perp$

$$\frac{\Delta\phi}{e}=-\frac{\mu_\perp N}{\varepsilon_0\varepsilon_r A}, \qquad (5)$$

where N/A is the number of sites per unit area.

We calculated dipole moments of the individual molecules (4-ATP, AT, and ATD) using quantum chemical techniques.[18] The results are listed in Table III. For our monolayers with a $(\sqrt{3}\times\sqrt{3})R30°$ structure, $N/A=4.8$

TABLE II. Results from Fig. 3: Parameters resulting from fits to trapezoidal barrier model.

	500 mV, 100 pA			500 mV, 200 pA			500 mV, 500 pA		
Sample	ϕ_t (eV)	ϕ_s (eV)	s (Å)	ϕ_t (eV)	ϕ_s (eV)	s (Å)	ϕ_t (eV)	ϕ_s (eV)	s (Å)
Au	2.27(2)	2.37(5)	7.81(3)	2.15(1)	2.32(3)	7.55(2)	2.44(1)	2.10(2)	6.89(1)
4-ATP	0.96(1)	3.60(4)	8.49(3)	0.96(2)	3.19(8)	8.23(5)	0.93(1)	3.87(4)	7.18(2)
AT	1.67(1)	2.53(4)	8.27(2)	1.82(1)	2.12(4)	8.00(3)	1.98(1)	1.86(3)	7.54(2)
ATD	0.34(1)	4.55(3)	8.46(3)	0.70(1)	4.09(4)	7.63(2)	0.52(1)	3.40(3)	7.88(2)

$\times 10^{18}$ molecules/m^2 and $\varepsilon_r = 2.4$[4]. This yields for the calculated dipoles (considering the component p_z along the molecules) a potential drop $\Delta\phi/e$ of -1.25, 0.20, and -1.28 V for 4-ATP, AT, and ATD, respectively. The sign of the barrier slope is consistent with the sign of the dipole moment. In particular, the near absence of a barrier slope in the AT molecule coincides well with the absence of an on-axis dipole moment for this molecule.

In addition to the dipole, which originates in the molecules, an interface dipole will be formed when the thiol forms a covalent bond with the gold substrate. Since the gold-sulfur distance is about 1.9 Å, and typical charge transfer is expected to be $-0.2e$ to $-0.4e$ from Au to S,[19] this would mean a dipole moment of 0.9 to 1.8 D and a potential drop of 0.7 to 1.4 V, respectively. It is difficult to estimate how important is the contribution of this Au-S dipole. Screening was suggested to be important by Campbell *et al.*,[7] and the contribution of the interface dipole was found to be small. In our experiments, apparently the contribution likewise is small.

The fit results yield effective tunnel barrier heights (which represent the distance between the gold Fermi level and the closest molecular orbital with significant coupling) of approximately 2 to 4 eV. This is consistent with work by Yoshimura *et al.*,[20] who found in optical measurements an absorption peak energy of 4.9 eV for TDA and and 2.9 eV for a copolymer of TDA and DAB. From *ab initio* calculations, Onipko *et al.* found a gap value of 5 eV for 4-ATP and 4.1 eV for ATD.[9]

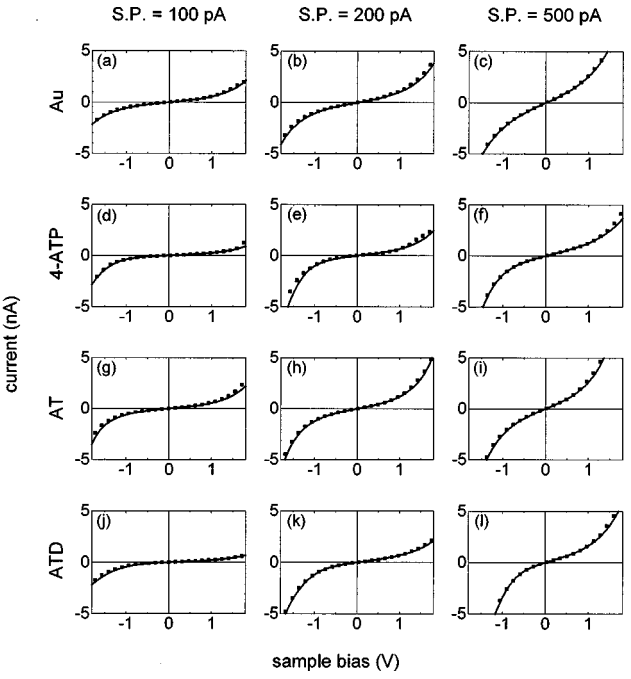

FIG. 7. Fits of Eq. (4) (solid lines) to the experimental results of Fig. 3 (squares). S.P. is the tunneling current setpoint (at 500 mV). (a)–(c) are for Au, (d)–(f) for 4-ATP, (g)–(i) for AT, and (j)–(l) for ATD.

The one-dimensional model that we have adopted to extract the barrier parameters is, in principle, a very simple one. The advantageous formulation based on a limited number of physical aspects (molecule length, effective barrier), makes the experimental system more transparent. Implicit factors like the dipole action can be made more explicit afterwards. Specific assumptions about the tip DOS are not needed. As such the simplified approach gives a more general picture of the impact of assembled molecules on tunneling. The error margins in Tables I and II give an indication for the correctness of the fit, within the constraints of the model. For small changes in the barrier shape, no large shifts in the fitted barrier parameters were observed indicating that the model can acceptably treat the experimental variations. In all cases, a trapezoidal shape is necessary to obtain a good agreement between experiment and fit.

The difference in ambient conditions (nitrogen vs air) does not seem to have a significant impact (Fig. 2 vs Fig. 3, and Fig. 5 vs Fig. 6, respectively). Only for gold is the barrier shape quite different, but this can be attributed to the measuring procedure: the nitrogen measurements (Fig. 2) were taken on a single spot, whereas for the air measurements (Fig. 3) the I-V curves were taken over a large area, thus resulting in an averaged and more reliable picture. The agreement between the observed I-V curves in air and nitrogen for the assembled molecules excludes the assumption that the always present capillary water film in the case of air ambient dominates. Instead, it may indicate that the molecules themselves are responsible for the observed behavior.

It is remarkable that all our fits result in a barrier thickness s of roughly 8 Å. The fits become significantly worse (χ^2 increases by more than an order of magnitude) when fixing s to the length of AT or ATD (13 and 19 Å, respectively). This implies that for the longer molecules the tip may be penetrating the molecular layer. In such a case, the transparency of the longer molecules is not large enough to allow sufficient current through the full length of the molecule (at least for the current setpoints, which are possible in our experiments). The possibly surprising aspect of our results is that the disorder that would be introduced by penetration of the tip apparently does not have a strong effect on the asymmetry introduced by the molecules. However, the fit results are obtained within the assumptions of our model of uniform DOS and $m = m_e$, which may be too restrictive. Especially

TABLE III. Calculated dipoles (*x,y,z* components) for 4-ATP, AT, and ATD from top to bottom. In the calculation the molecules are oriented in the positive *z* direction. The *z* component thus designates the dipole moment along the surface normal (as in Fig. 1) and will be important in the STM experiments.

Molecule	Dipole Direction	p_x	p_y	p_z
$\cdot$S-C_6H_4-NH_2	$-\rightarrow+$	0	0	1.659
$\cdot$S-C_6H_4-N=C^H-C_6H_4-C^H=O	$+\leftarrow-$	0.037	−1.482	−0.121
$\cdot$S-C_6H_4-N=C^H-C_6H_4-C^H=N-C_6H_4-NH_2	$-\rightarrow+$	−0.133	−1.073	1.693

an effective mass different from m_e would result in a different s (s scales with $1/\sqrt{m}$). Nevertheless, in Ref. 9, the tunneling behavior of this class of molecules is investigated from an *ab initio* point of view. Also there, it is concluded that the tip is penetrating in the molecules. As a function of setpoint, all molecules show a consistent decrease in the fitted barrier thickness with increasing setpoint current, irrespective of the ambient conditions. Only the result for ATD in air shows an increase in thickness for the highest setpoint current (500 pA). The change in the barrier tilt should not be regarded as a significant change in barrier heights (on one or both sides of the barrier) but rather as an indication for the inaccuracy in the fitted parameters.

On crystalline gold substrates, we observed symmetric as well as (sometimes) asymmetric STS $I(V)$ curves. Asymmetry is not expected from the barrier profile, since the work functions of both Au and Pt are approximately equal. Although generally on clean metal surfaces, no pronounced bias-voltage dependence is observed.[21] A surface state on the gold(111) surface at −0.4 eV has been found by Kaiser and Jaklevic, which resulted in an asymmetric dI/dV-V curve in STS.[22] Note that such a surface state cannot be the cause of the asymmetry at the 1.5 V scale, which we observe for our molecular films.

The observed large-voltage-scale asymmetry in some $I(V)$ curves on bare gold should probably be attributed to a variability in tip properties. If an impurity atom adsorbs onto a Pt/Ir tip, it will likely be charged positively. This results in a local-small dipole, reducing the work function, and in an enhanced density of *empty* states near the Fermi level, resulting in an enhanced current for negative sample voltage. This is indeed the type of asymmetry we observed. Because the effects of the molecular layers in STS were systematic and reproducible, in contrast to the results for bare gold, we think the interpretation of the molecular electronic structure is still appropriate. Perhaps the tip is generally somewhat cleaned of adsorbates when it penetrates the top of the monolayer film.

V. CONCLUSIONS

In conclusion, we have analyzed $I(V)$ spectra of self-assembled molecular monolayers of short conjugated molecules taken with STM. The molecules act as a potential barrier to electron transmission without resonances at least up to 1.5 V bias. This behavior is consistent with the gap in the density of states existing at the Fermi level of such molecules. The potential barrier is tilted due to permanent dipole moments in such molecules, giving rise to asymmetric $I(V)$ curves.

An important conclusion within the used model and the specific assumptions in the context of experiments on electronic transport through such molecules is that the fitted barrier thickness of less than 1 nm implies penetration of the STM in the thicker monolayers. This suggests that transfer of more than a few pA/s through a typical single conjugated molecule of length larger than 1 nm may be difficult, at least for voltages that we can apply without destroying the molecule.

ACKNOWLEDGMENTS

This work is part of the research program of the Dutch Foundation for Fundamental Research of Matter (FOM), which is financially supported by the Dutch Science Foundation (NWO). I.J.G. acknowledges support from the Royal Dutch Academy of Sciences (KNAW). We acknowledge very useful and stimulating discussions with A. Onipko, Yu. Klymenko, and Yu. Nazarov. We thank Bernard Rousseeuw for help with preparation of the samples.

*Present address: Philips Research Laboratories, Professor Holstlaan 4, 5656 AA Eindhoven, The Netherlands.

†Corresponding author. Email address: vanderdrift@dimes.tudelft.nl

‡Present address: Netherlands Institute for Metals Research, P.O. Box 5008, 2600 GA Delft, The Netherlands.

[1] See, e.g., H. Nejoh, Nature (London) **353**, 640 (1991); C. Joachim, J. K. Gimzewski, R. R. Schlittler, and C. Chavy, Phys. Rev. Lett. **74**, 2102 (1995); L. A. Bumm *et al.*, Science **271**, 1705 (1996); W. Tian *et al.*, J. Chem. Phys. **109**, 2874 (1998), and references therein.

[2] See, e.g., A. Aviram, C. Joachim, and M. Pomerantz, Chem. Phys. Lett. **146**, 490 (1988); V. Rousset, C. Joachim, B. Rousset, and N. Fabre, J. Phys. III **5**, 1985 (1995); C. J. Muller *et al.*, Nanotechnology **7**, 409 (1996); M. A. Reed, *et al.*, Science **278**, 252 (1997); early work on carbon nanotubes: S. J. Tans *et al.*, Nature (London) **386**, 474 (1997); M. Bockrath *et al.*, Science **275**, 1922 (1997); C. Zhou *et al.*, Appl. Phys. Lett. **71**, 611 (1997); C. Kuergeris *et al.*, Phys. Rev. B **59**, 12 505 (1999), and references therein.

[3] See, Philos. Trans. R. Soc. London, Ser. A **355**, 1725 (1997), and references therein.

[4] J. J. W. M. Rosink, M. A. Blauw, L. J. Geerligs, E. van der Drift, B. A. C. Rousseeuw, and S. Radelaar, Mater. Sci. Eng., C **8,9**, 275 (1999); J. J. W. M. Rosink, M. A. Blauw, L. J. Geerligs, E. van der Drift, B. A. C. Rousseeuw, S. Radelaar, W. G. Sloof, and E. J. M. Fakkeldij, Langmuir **16**, 4547 (2000).

[5] E. L. Wolf, *Principles of Electron Tunneling Spectroscopy* (Oxford University Press, New York, 1985).

[6] A. Dhirani, P.-H. Lin, P. Guyot-Sionnest, R. W. Zehner, and L.

R. Sita, J. Chem. Phys. **106**, 5249 (1997).
[7] I. H. Campbell, S. Rubin, T. A. Zawodzindski, J. D. Kress, R. L. Martin, and D. L. Smith, Phys. Rev. B **54**, R14 321 (1996); I. H. Campbell, J. D. Kress, R. L. Martin, and D. L. Smith, Appl. Phys. Lett. **71**, 3528 (1997).
[8] S. Datta, W. Tian, S. Hong, R. Reifenberger, J. I. Henderson, and C. P. Kubiak, Phys. Rev. Lett. **79**, 2530 (1997).
[9] A. I. Onipko, K.-F. Berggren, Yu. O. Klymenko, L. I. Malysheva, J. J. W. M. Rosink, L. J. Geerligs, E. van der Drift, and S. Radelaar, Phys. Rev. B **61**, 11 118 (2000).
[10] Y.-T. Kim, R. L. McCarley, and A. J. Bard, J. Phys. Chem. **96**, 7416 (1992).
[11] C. Schönenberger, J. A. M. Sondag-Huethorst, J. Jorritsma, and L. G. J. Fokkink, Langmuir **10**, 611 (1994); J. J. W. M. Rosink, M. A. Blauw, L. J. Geerligs, E. van der Drift, B. A. C. Rousseeuw, and S. Radelaar, Opt. Mater. **9**, 416 (1998).
[12] For each set of $I(V)$ curves, a possibly existing overall zero bias offset was substracted.
[13] W. F. Brinkman, R. C. Dynes, and J. M. Rowell, J. Appl. Phys. **41**, 1915 (1970).
[14] Yuli Nazarov (private communication).
[15] J. Bardeen, Phys. Rev. Lett. **6**, 57 (1961).
[16] J. Tersoff and D. R. Hamann, Phys. Rev. B **31**, 805 (1985).
[17] S. Gasiorowicz, *Quantum Physics* (Wiley, New York, 1974).
[18] GAUSSIAN 98W and MOPAC (Chem3D) resulted in the same dipole moments within about 20%. We followed the procedure of Campbell *et al.* (Ref. 7): First, the geometry of the thiols was obtained by minimizing the energy on a PM3 level. This was followed by a Hartree-Fock energy minimization using a STO-3G basis set. The thiol hydrogen was then removed and the dipole moment of the resulting radical is calculated using a more extensive 6-31*G* basis set.
[19] H. Sellers, A. Ulman, Y. Shnidman, and J. E. Eilers, J. Am. Chem. Soc. **115**, 9389 (1993).
[20] T. Yoshimura, S. Tatsuura, W. Sotoyama, A. Matsuura, and T. Hayano, Appl. Phys. Lett. **60**, 268 (1992).
[21] R. Wiesendanger, *Scanning Probe Microscopy and Spectroscopy* (Cambridge University Press, Cambridge, 1994).
[22] W. J. Kaiser and R. C. Jaklevic, IBM J. Res. Dev. **30**, 411 (1986).